Quantum Mechanics / Extremely Localized Molecular Orbital Embedding Strategy for Excited-States. 2. Coupling to the Equation-of-Motion Coupled Cluster Method

Giovanni Macetti[(1)], Alessandro Genoni[(1)*]

(1) Université de Lorraine & CNRS, Laboratoire de Physique et Chimie Théoriques (LPCT), UMR CNRS 7019, 1 Boulevard Arago, F-57078 Metz, France.

* Correspondence to:

Alessandro Genoni, Université de Lorraine & CNRS, Laboratoire de Physique et Chimie Théoriques (LPCT), UMR CNRS 7019, 1 Boulevard Arago, F-57078 Metz, France. E-mail: alessandro.genoni@univ-lorraine.fr; Phone: +33 (0)3 72 74 91 70; Fax: +33 (0)3 72 74 91 87.

ABSTRACT

Equation-of-Motion Coupled Cluster with single and double excitations (EOM-CCSD) is currently one of the most accurate quantum chemical methods for the investigation of excited-states, but its non-negligible computational cost unfortunately limits its application to small molecules. To extend its range of applicability, one possibility consists in its coupling with the so-called multi-scale embedding techniques. Along this line, in this work we propose the interface of the EOM-CCSD method with the recently developed quantum mechanics / extremely localized molecular orbital (QM/ELMO) strategy, an approach where the chemically relevant region of the investigated system is treated at fully quantum chemical level (QM region), while the remaining part (namely, the chemical environment) is described through transferred and frozen extremely localized molecular orbitals (ELMO subsystem). In order to determine capabilities and limitations of the novel EOM-CCSD/ELMO approach, some validation tests were properly designed and carried out. They indicated that the new approach is particularly useful and efficient in describing local electronic transitions in relatively large systems, for both covalently and non-covalently bonded QM and ELMO regions. In particular, it has been shown that, including only a limited number of atoms in the chemically active subunit, the ELMO-embedded computations enable the reproduction of excitation energies and oscillator strengths resulting from full EOM-CCSD calculations within the limit of chemical accuracy, but with a significantly reduced computational cost. Furthermore, despite the approximation of an embedding potential given by frozen extremely localized molecular orbitals, it was observed that the new strategy is able to satisfactorily account for the effects of the environment.

TOC GRAPHICS

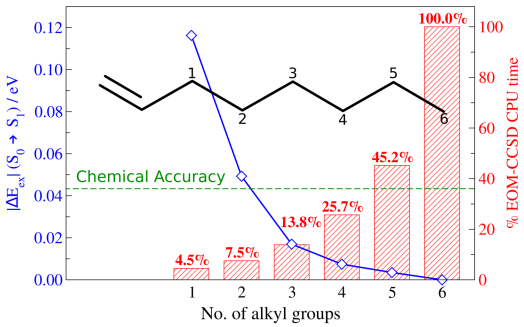

KEYWORDS: excited-states, embedding techniques, QM/QM' strategies, extremely localized molecular orbitals (ELMOs), Equation-of-Motion Coupled Cluster method

I. INTRODUCTION

Over the years, quantum chemistry has proposed different computational techniques to properly describe excited-states of molecules, ranging from simple and intuitive Δ-Self-Consistent Field (ΔSCF) approaches[1-4] to more elaborated multi-reference strategies[5-12].

When dealing with medium/large systems, Time-Dependent Density Functional Theory[13-15] (TDDFT) is usually the method of choice due to its favorable compromise between chemical accuracy and computational scaling (M^3/M^4, with M as the number of basis functions used in the calculation). However, although TDDFT works quite well for valence excitations, it is unfortunately characterized by some well-known flaws when, for example, it is used to describe Rydberg states, long-range charge-transfer excitations, conical intersections or double excitations.[16,17]

If one really wanted to achieve a very high accuracy in the computation of excited-state properties, it would be desirable to resort to methods based on correlated wave functions. In this context, Equation-of-Motion Coupled Cluster with single and double substitutions (EOM-CCSD) can be considered as the current gold standard technique,[18,19] although its unfavorable computational scaling (M^6) prevents a direct application to systems larger than about fifty atoms.

Different strategies have been proposed to extend the range of applicability of EOM-CCSD. Just to cite a few of them, we can mention the methods exploiting the local nature of atomic or molecular orbitals[20-24] or those techniques that were able to efficiently reduce the space of virtual orbitals[25,26]. However, to really apply the EOM-CCSD method to very large systems, the technique has to be coupled with embedding and/or multiscale strategies. In this context, we can consider the coupling of EOM-CCSD with molecular mechanics in QM/MM (quantum mechanics / molecular

mechanics) computations of excited-states or those investigations in which EOM-CCSD has been interfaced with implicit solvent models, such as PCM (polarizable continuum model).[27-29] Another interesting attempt is represented by the method proposed by Haldar and Dutta,[30] who very recently devised a fragment-based approach to broaden the applicability of the domain-based local pair natural orbital (DLPNO) implementation of the Equation-of-Motion Coupled Cluster method for the electron affinity (EA-EOM-CCSD).[31] Finally, and more importantly for the work that will be discussed in the present paper, EOM-CCSD has been also coupled with the successful projection-based embedding (PBE) technique[32-35] originally introduced jointly by the Manby and Miller research groups. Along this line, the first work is the one conducted by Bennie and coworkers,[36] who have practically extended the original version of PBE to EOM-CCSD and showed that their new embedding approach for excited-states is capable of providing results in excellent agreement with those obtained from the corresponding full EOM-CCSD computations. Furthermore, more recently Goodpaster and collaborators have interestingly exploited their absolutely localized version of the projection-based embedding strategy[37,38] to significantly reduce the computational cost of EOM-CCSD without impacting the accuracy of the results.[39] For the sake of completeness, it is worthwhile to remark that the PBE technique has been also successfully coupled with other quantum chemical methods for excited-states, such as TDDFT[39-42] and CASSCF[43] (Complete Active Space Self-Consistent Field).

In the framework of the strategies mentioned above, the goal of this work is to introduce the coupling of EOM-CCSD with the recent QM/ELMO (quantum mechanics / extremely localized molecular orbital) embedding strategy[44,45], a technique in which the crucial region of the system is treated with traditional quantum

chemical approaches, while the other part is described through transferred and frozen extremely localized molecular orbitals (ELMOs). In fact, ELMOs are molecular orbitals absolutely localized on small molecular subunits[46-48] and, for this reason, easily transferable from molecule to molecule[49-55.] In particular, given their reliable transferability, databanks of extremely localized molecular orbitals have been recently constructed[49,50,56] and exploited to almost instantaneously obtain approximate electron densities/wave functions of macromolecules and to successfully refine crystal structures of polypeptides and proteins[57].

The QM/ELMO approach has been developed both for single[44,45] (Hartree-Fock and Density Functional Theory) and multi-determinant[45] (particularly, Møller-Plesset perturbation theory and Coupled Cluster) techniques. The validation tests have indicated that, in practically all the situations, the results of the ground state QM/ELMO calculations agree with those of the corresponding fully QM computations within chemical accuracy (1 kcal/mol), with the former obtained at a much lower computational cost.[45] The computational advantage is particularly evident for post-HF/ELMO calculations due to the intrinsic reduction in the number of virtual molecular orbitals associated with the QM/ELMO embedding scheme (see the Theory section for more details).[45] This feature of the QM/ELMO approach is common to other fully quantum mechanical embedding methods, such as the above-mentioned absolutely localized PBE strategy introduced by the Goodpaster group[37,38] or other recent techniques proposed by Hammes-Schiffer *et al*.[58,59] and by Claudino and Mayhall[60]. Moreover, as one should expect, this characteristic is also very favorable in order to significantly reduce the computational cost of EOM-CCSD calculations, as we will show below and as it was also stressed for the absolutely localized PBE strategy for excited-states[39].

The present paper is organized as follows. In Section II, we will present the basic theoretical features of the QM/ELMO philosophy and we will discuss how the environment effects are or can be possibly taken into account in the EOM-CCSD/ELMO approach. In section III, we will describe the validation tests that were performed to evaluate the capabilities of the new technique. The obtained results will be afterwards shown and discussed in section IV, which will be followed by some general conclusions in section V. The main goal of the study is to introduce the EOM-CCSD/ELMO method and to prove that the novel strategy is able to accurately and cheaply describe localized excitations in relatively large systems, both in situations in which the QM and ELMO regions are divided across covalent bonds and in cases in which the frontier is between non covalently bonded subsystems (e.g., a solute surrounded by solvent molecules). Furthermore, the performed validation tests also aimed at assessing current capabilities and limitations of the developed method in taking into account the effects of the environment.

II. THEORY

II.A The QM/ELMO algorithm. In this subsection, we will describe the fundamentals of the QM/ELMO embedding scheme and particularly of the QM/ELMO self-consistent field (SCF) algorithm, which was the preliminary step to obtain occupied and virtual molecular orbitals used in the EOM-CCSD/ELMO calculations carried out in the present work.

The QM/ELMO method starts with the partitioning of the system under exam into the QM and ELMO regions. The former corresponds to the chemically important part of the system, while the latter represents the chemical environment. Extremely localized molecular orbitals are transferred to the ELMO region from the constructed libraries[56]

or from tailor-made model molecules by exploiting the rotation/transfer strategy proposed by Philipp and Friesner[49,61] in the context of QM/MM approaches that use strictly localized bond orbitals (SLBOs) to describe the frontier between the QM and MM subsystems. For more details about theory, transfer and libraries of ELMOs, we refer the readers to the papers on the construction of the ELMO databanks[49,50,56] or to the Supporting Information of our related work about the TDDFT/ELMO approach[62].

Before starting the actual QM/ELMO SCF algorithm, a preliminary orthogonalization procedure on the basis functions of the QM region and on the exported ELMOs is carried out. It consists in i) Löwdin orthonormalizing the transferred extremely localized molecular orbitals, ii) projecting out the orthonormalized ELMOs from the basis functions of the QM region, and iii) canonically orthogonalazing the QM basis functions obtained at point (ii). These three steps can be summarized through the following transformation:

$$\boldsymbol{\chi}' = \boldsymbol{\chi}\,\mathbf{B} \quad (1)$$

where $\boldsymbol{\chi}$ is the starting $1 \times M$ array $[|\chi_1\rangle, |\chi_2\rangle, \dots, |\chi_M\rangle]$ of the non-orthogonal basis functions for the whole system, $\boldsymbol{\chi}'$ is the final $1 \times M_{QM}$ array $[|\chi'_1\rangle, |\chi'_2\rangle, \dots, |\chi'_{M_{QM}}\rangle]$ of the final orthonormal basis functions for the QM subunit (with M_{QM} much lower than M), and $\mathbf{B}$ is a global $M \times M_{QM}$ transformation matrix that has a central role in the QM/ELMO SCF algorithm (full details about the orthogonalization procedure can be also found in the original works about the QM/ELMO approach[44,45] or in the Supporting Information of the related paper on the TDDFT/ELMO technique[62]).

Afterwards, the real self-consistent field procedure begins and it can be schematized through the following steps:

1. Determination of the $M \times M$ Fock matrix $\mathbf{F}$ in the original and non-orthogonal basis $\boldsymbol{\chi}$.

2. Transformation of matrix $\mathbf{F}$ to the $M_{QM} \times M_{QM}$ Fock matrix $\mathbf{F}'$ for the QM subsystem in the orthogonal basis $\boldsymbol{\chi}'$ by exploiting the transformation $\mathbf{F}' = \mathbf{B}^{\dagger}\mathbf{F}\,\mathbf{B}$, where $\mathbf{B}^{\dagger}$ corresponds to the transpose of the transformation matrix $\mathbf{B}$ seen in equation (1).
3. Diagonalization of matrix $\mathbf{F}'$ to obtain the coefficients of the (occupied and virtual) molecular orbitals of the QM region: $\mathbf{F}'\mathbf{C}' = \mathbf{C}'\,\mathbf{E}'$.
4. Transformation of the obtained molecular orbitals in the original and non-orthogonal basis $\boldsymbol{\chi}$ through the relation $\mathbf{C} = \mathbf{B}\,\mathbf{C}'$.
5. Determination of the QM one-particle density matrix: $\mathbf{P}^{QM} = \mathbf{C}\mathbf{C}^{\dagger}$.
6. Inspection of convergence on energy and density matrix. If convergence is reached, the SCF cycle ends, otherwise it restarts from point 1 where the one-particle density matrix $\mathbf{P}^{QM}$ at point 5 is used to update the Fock matrix $\mathbf{F}$.

It is worth noting that, since $M_{QM} \ll M$ (we remind that M is the number of basis functions for the whole system), the QM/ELMO methods are characterized by a significant reduction of the computational cost, especially if one deals with very large systems and if post-HF techniques are used to treat the QM region. In fact, assuming to work with a *2N*-electron closed-shell QM subsystem, the diagonalization at point 3 of the above-discussed SCF cycle provides N doubly occupied molecular orbitals (with N generally much lower than $N + N_{ELMO}$) and $M_{QM} - N$ virtual molecular orbitals (with $M_{QM} - N$ always much lower than $M - N$). Since the computational cost of correlated calculations for ground and excited-states depends on the number of occupied molecular orbitals and, even more importantly, on the number of the virtual ones (e.g., CCSD(T) and EOM-CCSD calculations scale as o^3v^4 and o^2v^4, respectively, with o and v as the number of occupied and virtual molecular orbitals), it is clear that the reduced dimensions of matrix $\mathbf{F}'$ entail important savings in terms

of CPU time, as already shown by means of preliminary validation tests on the QM/ELMO strategy. [45]

Therefore, on the basis of the property just discussed above, we decided to exploit the smaller set of occupied and virtual molecular orbitals obtained from the QM/ELMO SCF cycle in order to significantly reduce the computational cost of EOM-CCSD calculations. As previously mentioned in the Introduction, this philosophy is similar to the one adopted by Goodpaster and coworkers, who also coupled their absolutely localized variant of the PBE strategy to the Equation-of-Motion Coupled Cluster technique.[39]

The QM/ELMO algorithm described in this section and its coupling to EOM-CCSD have been implemented by properly modifying the relevant subroutines of the fully quantum mechanical methods in the quantum chemistry suite of programs *Gaussian09*.[63]

II.B Environment effects. In this subsection we will briefly discuss how the effects of the environment are or can be possibly taken into account in the EOM-CCSD/ELMO calculations of excited-states.

First of all, following Wen *et al*.,[39] the environment effects can be distinguished in ground state polarization and polarization response effects. In our case, the ground state polarization effects are simply given by the embedding potential provided by transferred extremely localized molecular orbitals. Compared to the projection-based embedding approaches for excited-states,[39] our treatment of the ground state polarization is only approximate and not flexible. In fact, while in the PBE-based techniques the embedding potentials for the excited-states are generally constructed from the converged DFT ground state electron densities of the whole system or of its

subunits, in our EOM-CCSD/ELMO strategy the embedding potential is represented by transferred ELMOs that remain frozen throughout the preliminary HF/ELMO calculation and that, therefore, are not influenced by the actual ground state electron density of the QM region (it is worth reminding that HF/ELMO or DFT/ELMO calculations are always preliminary steps to carry out QM/ELMO calculations for excited-states). The advantage of our technique is that the transfer of extremely localized molecular orbitals to the environment region is practically instantaneous and it is not necessary to perform a preliminary DFT calculation on the whole molecule under exam. In the future, a possible way to increase the flexibility of the ELMO-based methods might consist in further developing polarizable QM/ELMO techniques in which transferred virtual extremely localized molecular orbitals might be used to relax the electronic structure / electron density of the environment (i.e., the ELMO region) as a response to the influence of the ground state electron distribution of the chemically active subsystem.

Concerning the polarization response of the environment, in analogy with the absolutely localized version of the PBE approach for excited-states,[39] also the EOM-CCSD/ELMO technique does not intrinsically take into account this effect. There are three possibilities to introduce it: i) including more atoms or molecular orbitals in the active QM region; ii) exploiting a state-averaged approach, as proposed by the Carter[64] and Goodpaster[39] groups; iii) adding a suitable TDDFT correction. As it will be shown below, the first and the third options are those that have been tested in the present work.

The first possibility is the most straightforward, but potentially also the most expensive from the computational point of view. In our case, this option consists in properly selecting a set of originally frozen ELMOs, removing them from the ELMO

region and treating the associated electrons in the QM subsystem explicitly. This is also the strategy that has been adopted when the conventional projection-based embedding technique[32-35] (not its absolutely localized variant[37,38]) was coupled with wavefunction-based methods for excited-states. In that case, polarization response has been quite easily taken into account by including a certain number of relevant occupied localized molecular orbitals (and consequently the corresponding electrons) of the environment region in the QM subsystem.[36]

The second possibility would consist in developing a self-consistent strategy to relax the ELMO electron density by taking into account the ground state and excited-states electron distributions of the QM region. As indicated above for the ground state polarization, this task might be accomplished in the future by developing a technique that exploits transferred virtual ELMOs.

Finally, following Wen *et al.*,[39] the third option is equivalent to write the excitation energy as follows:

$$\widetilde{\omega}_{\mathrm{EOM-CCSD/ELMO}} = \omega_{\mathrm{EOM-CCSD/ELMO}} + \omega_{\mathrm{TDDFT}} - \omega_{\mathrm{TDDFT/ELMO}} \qquad (2)$$

where $\widetilde{\omega}_{\mathrm{EOM-CCSD/ELMO}}$ is the embedded EOM-CCSD/ELMO excitation energy after the TDDFT correction, $\omega_{\mathrm{EOM-CCSD/ELMO}}$ is the embedded EOM-CCSD/ELMO excitation energy before the TDDFT correction (including only the approximate ground state polarization), ω_{TDDFT} is the traditional TDDFT excitation energy on the full system, and $\omega_{\mathrm{TDDFT/ELMO}}$ is the embedded TDDFT excitation energy obtained through the recently developed TDDFT/ELMO strategy[62]. Of course, from the computational perspective, this option is convenient only if the cost of the full TDDFT computation is small compared to the one associated with the corresponding full EOM-CCSD calculation.

An investigation on the capabilities of the new EOM-CCSD/ELMO method in accounting for the environment effects will be described and discussed in subsections III.C and IV.B.

III. VALIDATION TESTS: COMPUTATIONAL DETAILS

As done for the recently proposed TDDFT/ELMO strategy,[62] also the EOM-CCSD/ELMO method underwent a series of validation tests previously carried out to assess capabilities and performances of other embedding variants of the EOM-CCSD technique (particularly of those based on the projection-based embedding approach[36,39]). All these validation tests will be described below, while the obtained results will be shown and discussed in Section IV.

For the sake of completeness, it is worth noting that almost all the computations in this work were carried out exploiting the *Gaussian09* software[63] in its standard version or in a modified variant where the new embedding techniques EOM-CCSD/ELMO and TDDFT/ELMO for excited-states were implemented. The only exceptions were the calculations and transfers of the ELMOs to be used in the QM/ELMO computations (see subsection III.D). In fact, for the calculations of tailor-made ELMOs we used a modified version of the GAMESS-UK package[65] where the Stoll equations[46] for the ELMOs determination were properly coded[47]; for the ELMOs transfers we exploited the *ELMOdb* program,[56] which is the software associated with the recently constructed ELMO libraries and which implements the rotation strategy for strictly localized molecular orbitals introduced by Philipp and Friesner[61].

Finally, if not differently specified, in this work all the EOM-CCSD and EOM-CCSD/ELMO computations were performed with basis-set aug-cc-pVDZ.

III.A EOM-CCSD/ELMO calculations with a covalent frontier. As first standard validation test, we decided to assess the convergence of EOM-CCSD/ELMO calculations as a function of the QM region size when the frontier between the QM and the ELMO subsystems coincides with a covalent bond. To accomplish this task, we considered two molecules characterized by a relatively long hydrocarbon chain: 1-octene and octanoic acid (see Figure 1), whose geometries were preliminarily optimized at B3LYP/cc-pVDZ level. The geometries were subsequently exploited to carry out full EOM-CCSD computations. For each molecule, the first three transitions were taken into account and the excitation energies and the oscillator strengths resulting from the full EOM-CCSD calculations were afterwards used as benchmark values.

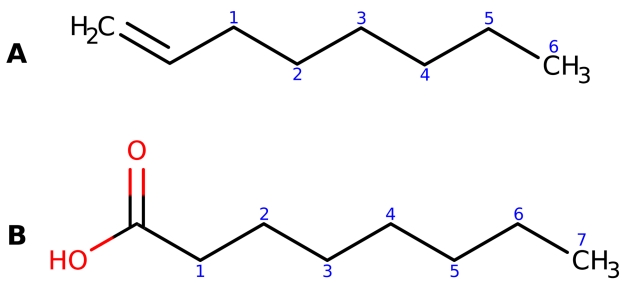

Figure 1. Schematic representation of the long-chain hydrocarbons considered for the test calculations: (A) 1-octene, and (B) octanoic acid. The numbers indicate the labels of the alkyl groups gradually added to the QM region.

Pertaining to the EOM-CCSD/ELMO computations, we gradually increased the size of the QM region by including the alkyl groups of the hydrocarbon chain together with the terminal functional group of the considered molecules (i.e., carboxylic group for octanoic acid and carbon-carbon double bond for 1-octene). Also for these calculations we took into account excitation energies and oscillator strengths associated with the first three excitations. The obtained values were compared to the reference ones resulting from the full EOM-CCSD computations mentioned above.

III.B EOM-CCSD/ELMO calculations with a non-covalent frontier. As second step, we decided to investigate the convergence of embedded EOM-CCSD/ELMO computations in cases of non-covalent frontiers between the QM and ELMO regions. To this purpose we investigated the case of four different molecules solvated by water: formaldehyde, acetaldehyde, acrolein and acrylamide.

For each of the above-mentioned systems, we initially carried out a preliminary Molecular Dynamics (MD) simulation (see Supporting Information for more details), from which we extracted a frame where the solute establishes two plausible hydrogen bond contacts with the surrounding water molecules. Considering that frame, we kept only the solute and the six closest solvent molecules (see Figure 2). The resulting systems were then used to perform benchmark full EOM-CCSD calculations. In analogy with the test calculations performed on their methods by Bennie *et al*.[36] and by Goodpaster and coworkers[39], also in our case we focused only on the $n \rightarrow \pi^*$ transition (first excited-state).

Concerning the EOM-CCSD/ELMO computations, we gradually enlarged the QM region by including the surrounding solvent subunits: in the cheapest EOM-CCSD/ELMO calculations, only the solute was included in the QM subsystem; we afterwards performed EOM-CCSD/ELMO computations by adding to the QM region only the two water molecules establishing hydrogen bond contacts with the solute; finally, we sequentially included the remaining water molecules by considering their distance from the oxygen atom of the carbonyl group of the solute molecule (formaldehyde, acetaldehyde, acrolein or acrylamide) taken into account. The excitation energies and the oscillator strengths for the $n \rightarrow \pi^*$ excitation resulting from the EOM-CCSD/ELMO calculations were then compared to the corresponding benchmark EOM-CCSD values.

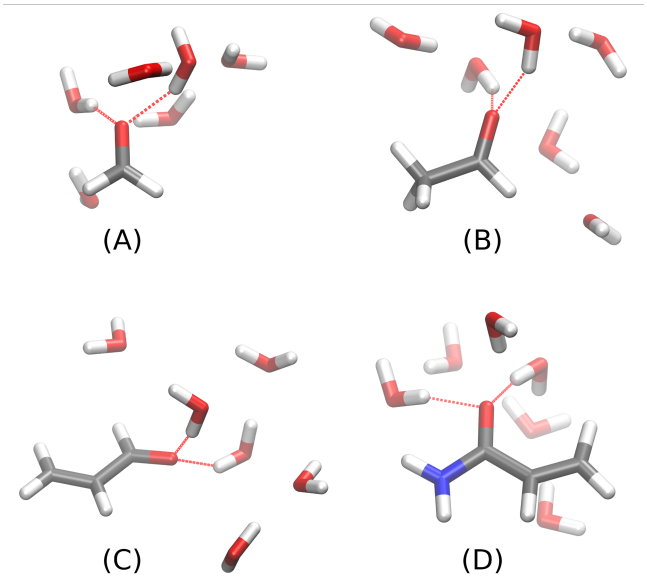

Figure 2. Solvated (A) formaldehyde, (B) acetaldehyde, (C) acrolein and (D) acrylamide: each system corresponds to the solute molecule surrounded by the six closest water molecules, as extracted from the chosen Molecular Dynamics simulation-frame. The red-dashed lines indicate the hydrogen bond contacts between the water molecules and the solute.

III.C Environment effects. In order to assess the capabilities of the new embedding method in accounting for the effects of the environment, we considered two of the molecules taken into account in the previous subsection: formaldehyde and acrylamide. For both of them, from the same MD simulation-frame used for the test calculations described above, we extracted the geometry of the system consisting of the solute and of the two water molecules involved in hydrogen bond contacts. We then performed the following calculations: i) traditional EOM-CCSD computations on the full system, which account for ground state polarization and polarization response; ii) traditional EOM-CCSD calculation on the solute molecule only, which does not account for any environment effect; iii) EOM-CCSD/ELMO computation on the full system with only the solute molecule in the QM region, which should include only an approximate ground state polarization; iv) EOM-CCSD/ELMO calculation as the previous one, but with the additional inclusion of properly selected ELMOs/electrons

in the QM region (see subsection IV.B for more details) to partially account for the polarization response; iv) TDDFT and TDDFT/ELMO (with only the solute molecules in the QM region) computations on the full system to determine the TDDFT corrections for the polarization response according to equation (2). Again, we considered only the excitation energies obtained for the $n \rightarrow \pi^*$ transition.

Finally, to conclude the investigation on the effects due to the environment, for both formaldehyde and acrylamide, we monitored the variation of the $n \rightarrow \pi^*$excitation energy as a function of the number of surrounding water molecules when the following type calculations are carried out: i) EOM-CCSD(0)/ELMO, namely an ELMO-embedded EOM-CCSD computation without water molecules in the QM region; ii) EOM-CCSD(2)/ELMO, namely an ELMO-embedded EOM-CCSD computation with two water molecules in the QM subsystem; iii) traditional TDDFT (CAM-B3LYP functional); iv) traditional Time-Dependent Hartree-Fock (TDHF). All the calculations were performed with basis-set aug-cc-pVDZ and the global number of water molecules was gradually increased from 2 to 30 taking into account their distance from the oxygen atom of the carbonyl group (see Figure S1 in the Supporting Information) and always using the MD simulation-frames considered for the benchmark tests described in subsection III.B.

III.D. ELMO calculations. For the computations of the extremely localized molecular orbitals to be used in the validation tests on octanoic acid and 1-octene (subsection III.A), the ELMOs of the alkyl groups were determined on the butane molecule exploiting the aug-cc-pVDZ basis-set on a geometry optimized at B3LYP/cc-pVDZ level. Pertaining to the test calculations on solvated formaldehyde, acetaldehyde, acrolein and acrylamide (see subsections III.B and III.C), we only

needed ELMOs to describe the surrounding water molecules and they were computed with basis-set aug-cc-pVDZ, always on a geometry optimized at B3LYP/cc-pVDZ level.

IV. RESULTS AND DISCUSSION

IV.A Convergence of the EOM-CCSD/ELMO calculations. In this subsection, we will analyze the convergence of the EOM-CCSD/ELMO calculations as a function of the size of the quantum mechanical region: at first, we will focus on the QM/ELMO computations with a frontier occurring at a covalent bond between the QM and the ELMO subsystems; afterwards we will consider the results of the QM/ELMO calculations with a non-covalent boundary between the two subunits. Finally, the cost of the performed EOM-CCSD/ELMO computations will be discussed.

First of all, let us consider the results for the first three excited-states of 1-octene and let us analyze the obtained excitation energies (see Figure 3A). We can notice that, for all the three electronic transitions, the EOM-CCSD/ELMO excitation energies clearly converge towards the fully EOM-CCSD ones, with the $|\Delta E_{ex}|$ discrepancies that start being lower than 0.043 eV (chemical accuracy threshold) when at least three alkyl groups are included in the QM region. This result can be interpreted considering the natural transition orbitals (NTOs) analysis associated with the full EOM-CCSD calculation on 1-octene (see Figure S2 in the Supporting Information), from which we can evince that the extent of localization for the first three excited-states is practically equivalent. Pertaining to the oscillator strengths (see Figure 3B), a gradual convergence of the EOM-CCSD/ELMO values towards the reference fully quantum mechanical ones is also observed. For this quantity, convergence is faster for the first excited-state, while for the $S_0 \rightarrow S_2$ and $S_0 \rightarrow S_3$ transitions a *plateau* is reached when

four alkyl moieties are included in the QM subsystem, although it is also worth noting that the oscillator strengths obtained for the $S_0 \rightarrow S_2$ excitation are one order of magnitude smaller than those obtained for the $S_0 \rightarrow S_3$ transition (see details in the caption of Figure 3 and also Tables S1 and S2 in the Supporting Information for the actual values of excitation energies and oscillator strengths obtained for 1-octene).

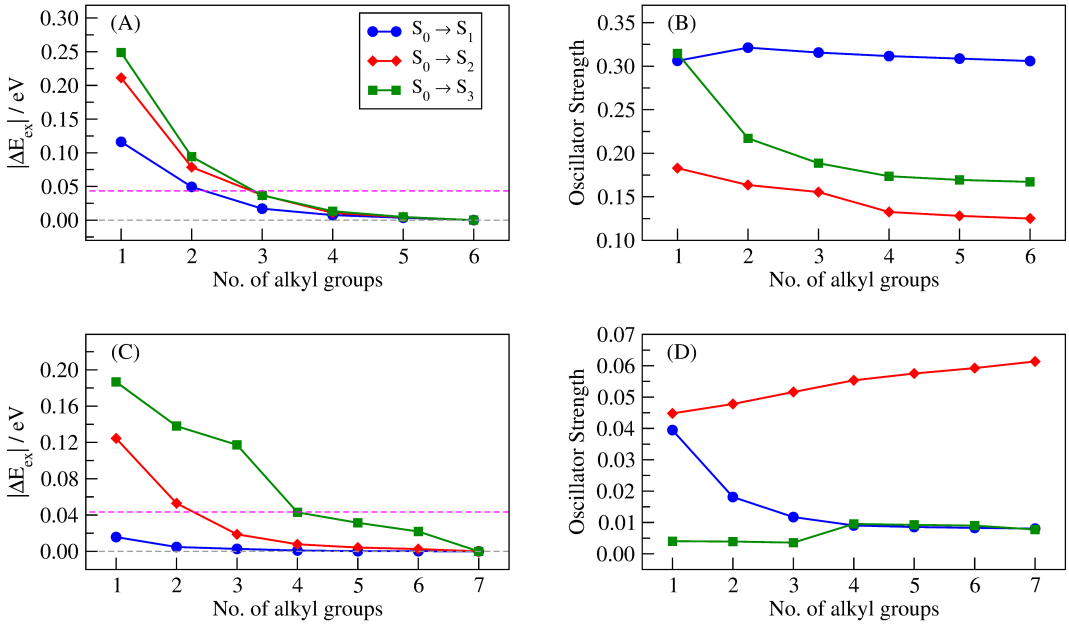

Figure 3. Results of the full EOM-CCSD and EOM-CCSD/ELMO calculations on 1-octene and octanoic acid for their first three excited-states: (A) absolute discrepancies between the EOM-CCSD and EOM-CCSD/ELMO excitation energies of 1-octene; (B) oscillator strengths of 1-octene (the $S_0 \rightarrow S_1$ and $S_0 \rightarrow S_2$ values are multiplied by 10; for all the transitions, the benchmark EOM-CCSD values are those obtained for six alkyl groups in the QM region); (C) absolute discrepancies between the EOM-CCSD and EOM-CCSD/ELMO excitation energies of octanoic acid; (D) oscillator strengths of octanoic acid (the $S_0 \rightarrow S_1$ values are multiplied by 100; for all the transitions, the benchmark EOM-CCSD values are those obtained for seven alkyl groups in the QM subsystem). The magenta-dashed lines in (A) and (C) indicates the chemical accuracy threshold.

Now, let us analyze the results obtained for octanoic acid. Concerning the excitation energies (see Figure 3C), the EOM-CCSD/ELMO values converge to the fully quantum mechanical results as the size of the QM region increases, regardless of the

considered excited-state. Nevertheless, while for the first transition $S_0 \rightarrow S_1$ the discrepancy with respect to the EOM-CCSD value is already well below 0.043 eV when only one alkyl group is included in the quantum mechanical subsystem (discrepancy of 0.016 eV), in the other two cases the convergence towards chemical accuracy is slower. In particular, for transitions $S_0 \rightarrow S_2$ and $S_0 \rightarrow S_3$, the $|\Delta E_{ex}|$ discrepancy starts being lower than or equal to the chemical accuracy threshold when at least 3 and 4 alkyl groups are considered in the QM subunit, respectively. This can be explained again considering the extent of localization for the different excitations. In fact, from the inspection of the NTOs associated with the full EOM-CCSD calculation for the first three excited-states of octanoic acid (see Figure S3 in the Supporting Information) it can be easily noticed that transition $S_0 \rightarrow S_1$ is well localized, while excitations $S_0 \rightarrow S_2$ and $S_0 \rightarrow S_3$ are gradually more delocalized over the examined molecule. Convergence is also observed for the oscillator strengths. From Figure 3D, we can see that, for the first ($S_0 \rightarrow S_1$) and third ($S_0 \rightarrow S_3$) excitations, the EOM-CCSD/ELMO values practically reach a *plateau* when four alkyl groups are treated at quantum mechanical level, with the differences that, for transition $S_0 \rightarrow S_1$, the trend is monotonically decreasing and the obtained oscillator strengths are two order of magnitude lower than those observed for transition $S_0 \rightarrow S_3$ (see details in the caption of Figure 3). Concerning the second ($S_0 \rightarrow S_2$) excited-state, the values of the oscillator strength resulting from the EOM-CCSD/ELMO computations gradually approach the EOM-CCSD one with a monotonically increasing trend as the size of the QM region becomes larger, although in this case a clear *plateau* is not reached (actual values of excitation energies and oscillator strengths for octanoic acid are also respectively given in Tables S1 and S2 of the Supporting Information).

The main results of the test calculations on the systems without covalent frontier between the QM and ELMO regions are summarized in Figure 4, where we graphically reported the absolute deviations of the EOM-CCSD/ELMO $n \rightarrow \pi^*$ excitation energies from the benchmark EOM-CCSD values as a function of the size of the QM subsystem (see also Tables S3 and S4 in the Supporting Information for the actual values of the excitation energies and of the corresponding oscillator strengths). It is possible to notice that, in practically all the cases, the discrepancy is already below the chemical accuracy limit when only the solute molecule is included in the QM region and all the surrounding water molecules belong to the ELMO subsystem. In particular, for formaldehyde and acrylamide, the initial $|\Delta E_{ex}|$ deviations are already very small (0.010 eV and 0.008 eV, respectively) and indicate the reliability of the description of the environment at the approximate ELMO level. This is even more worthy considering the fact that the corresponding gas-phase calculations provide excitation energies that are quite far from those obtained in presence of the six surrounding water molecules, with absolute discrepancies that amount to 0.285 eV and 0.619 eV for formaldehyde and acrylamide, respectively. In the other two cases (acetaldehyde and acrolein), the excitation energy values resulting from EOM-CCSD/ELMO calculations with all the water molecules in the ELMO region are slightly below 0.043 eV (0.033 eV and 0.040 eV for acetaldehyde and acrolein, respectively). However, increasing the size of the QM subsystem, the situation significantly improves, with discrepancies that drop below 0.007 eV when only the two water molecules involved in hydrogen bonds are treated in a fully quantum mechanical way.

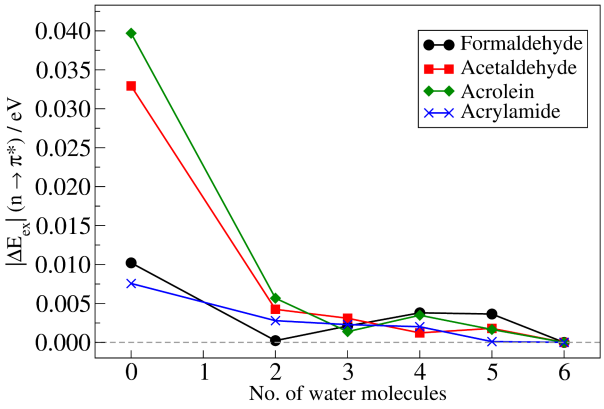

Figure 4. Absolute discrepancies between the EOM-CCSD and EOM-CCSD/ELMO excitation energies corresponding to the $n \rightarrow \pi^*$ transitions for solvated formaldehyde, acetaldehyde, acrolein, and acrylamide as a function of the QM region size.

Concerning the obtained oscillator strengths, the EOM-CCSD/ELMO computations provided values that are completely comparable to and, above all, almost always of the same order of magnitude of those obtained through the full EOM-CCSD method (see again Table S4 in the Supporting Information). In the graphs reporting the values of the oscillator strengths as a function of QM region size (see Figure 5), we can always notice a clear increase when the number of water molecules treated at fully quantum mechanical level rises from zero to two, after which the oscillator strengths converge towards the benchmark EOM-CCSD values. In all the examined cases, a *plateau* value is practically reached when two solvent molecules are included in the QM subsystem.

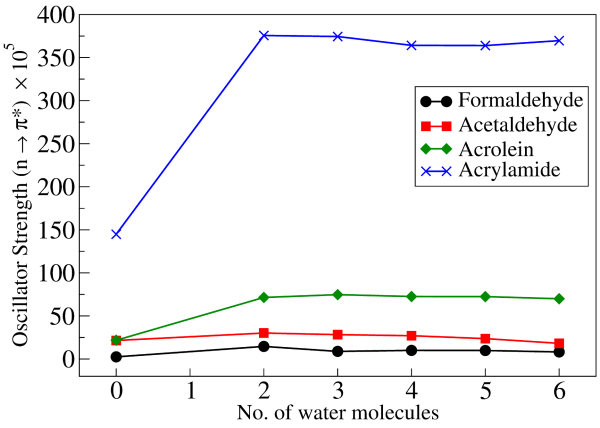

Figure 5. Oscillator strengths corresponding to the $n \rightarrow \pi^*$ transitions for solvated formaldehyde, acetaldehyde, acrolein, and acrylamide as a function of the QM region size. The reference EOM-CCSD values are those obtained for six water molecules in the QM region.

To conclude this section, we focus on the computational cost of the performed EOM-CCSD/ELMO calculations. For this purpose, in Tables 1 and 2 we provided the number of (frozen and active) occupied molecular orbitals, the number of active virtual orbitals and the CPU times corresponding to the EOM-CCSD/ELMO and full EOM-CCSD calculations performed on 1-octene (Table 1) and acrylamide (Table 2). Analyzing the collected data, we can clearly observe that the number of active occupied molecular orbitals and virtual molecular orbitals used in the EOM-CCSD/ELMO computations are significantly lower than those in the reference EOM-CCSD calculations, especially when the size of the QM region remains quite small. As already mentioned in the Introduction and in the Theory section, this directly affects the computational cost of the ECOM-CCSD/ELMO calculations, which are characterized by important reductions in terms of CPU time. For example, in Table 1 we can observe that when only three alkyl groups of 1-octene are included in the QM region (which allows to reach chemical accuracy for the first three excited-states), the EOM-CCSD/ELMO computation takes only 13.8% of the time taken by the

corresponding full EOM-CCSD calculation. Similar computational costs are observed for the excited-state computations performed on solvated acrylamide (see Table 2), for which we can notice that when the QM subsystem consists only of the solute and two water molecules, the CPU time is only 8.4% of the one recorded for the corresponding full quantum mechanical calculation. Finally, as expected, from Tables 1 and 2 we can see that the computational cost of the EOM-CCSD/ELMO calculations gradually increases with the size of the QM subunit. However, we can also observe that, for the EOM-CCSD/ELMO computations on 1-octene and solvated acrylamide, the recorded CPU times never exceed 45.2% and 44.4%, respectively, of the CPU times reported for the benchmark fully QM calculations. Completely analogous trends were observed for the computations carried out on the other systems taken into account in our validation tests (see Tables S5-S8 in the Supporting Information).

Table 1. Number of (frozen and active) occupied molecular orbitals (N_{occ}), number of virtual molecular orbitals (N_{virt}) and timings associated with the EOM-CCSD/ELMO and EOM-CCSD calculations (aug-cc-pVDZ basis-set) performed on 1-octene.[a, b]

Calculations	N_{occ}		N_{virt}	CPU time (s)	%
	Frozen	Active			
QM(1)/ELMO	24	8	109	16287.7	4.55
QM(2)/ELMO	21	11	148	26859.0	7.51
QM(3)/ELMO	18	14	187	49505.8	13.84
QM(4)/ELMO	15	17	226	91836.9	25.68
QM(5)/ELMO	12	20	265	161605.8	45.19
Full QM	8	24	312	357605.1	100.00

[a] The acronym QM(*N*)/ELMO indicates that *N* alkyl groups were included in the QM region for the EOM-CCSD/ELMO calculation; [b] the recorded timings were obtained by performing parallel calculations on 16 Intel Xeon Gold 6130 2.1 GHz processors.

Table 2. Number of (frozen and active) occupied molecular orbitals (N_{occ}), number of virtual molecular orbitals (N_{virt}) and timings associated with the EOM-CCSD/ELMO and EOM-CCSD calculations (aug-cc-pVDZ basis-set) performed on acrylamide surrounded by six water molecules.[a, b]

Calculations	N_{occ}		N_{virt}	CPU time (s)	%
	Frozen	Active			
QM(0)/ELMO	35	14	151	53498.0	2.36
QM(2)/ELMO	27	22	227	189200.3	8.35
QM(3)/ELMO	23	26	265	345155.1	15.22
QM(4)/ELMO	19	30	303	569756.8	25.13
QM(5)/ELMO	15	34	341	1006533.1	44.40
Full QM	11	38	379	2267035.0	100.00

[a] The acronym QM(*N*)/ELMO indicates that *N* water molecules were included in the QM region for the EOM-CCSD/ELMO calculation; [b] the recorded timings were obtained by performing parallel calculations on 16 Intel Xeon Gold 6130 2.1 GHz processors.

IV.B. Effects of the environment. The results of the test calculations to assess the capabilities of the EOM-CCSD/ELMO approach in taking into account the effects of the environment are reported in Table 3. Let us initially focus on the validation tests performed on formaldehyde. We can notice that, by including the two hydrogen-bonded water molecules in the ELMO region, the EOM-CCSD/ELMO method is able to satisfactorily take into account the environment effects, practically recovering completely the difference between the $n \rightarrow \pi^*$ excitation energy of formaldehyde in gas phase and the $n \rightarrow \pi^*$ excitation energy obtained for the solvated system (i.e., formaldehyde plus two water molecules) at full EOM-CCSD level. In particular, the discrepancy drops from -0.169 eV to 0.010 eV. However, we can observe that the EOM-CCSD/ELMO description slightly overestimates the benchmark value and this might be ascribed to the concurrence of two different factors: i) the approximate description of the ground state polarization through the embedding potential given by

frozen ELMOs; ii) the complete lack of polarization response. As already mentioned in the Computational Details section, to further improve the EOM-CCSD/ELMO description, and particularly to try to partially introduce the polarization response effects, we have adopted and tested two different strategies. One consisted in introducing a TDDFT-based correction, as indicated by equation (2) in the Theory section. The results are shown in Table 3 and indicate that this strategy strongly depends on the adopted functional. In fact, it provides better agreements with the full EOM-CCSD benchmark value when functionals CAM-B3LYP and PBE0 are used (perfect agreement and discrepancy of 0.004 eV, respectively), while a worsening is observed when functional B3LYP is adopted (deviation of -0.030 eV). The other possible approach consisted in including properly chosen ELMOs/electrons in the QM region, as also done by Bennie and coworkers in their coupling of the EOM-CCSD method with the projection-based embedding technique[36]. To evaluate this option, we thus performed an additional EOM-CCSD/ELMO calculation where we included in the QM subsystem eight additional electrons of the surrounding water molecules. In the initial EOM-CCSD/ELMO computation, four of these electrons had been described through ELMOs localized on the O-H bonds involved in the hydrogen bonds with formaldehyde; the other four had been described through ELMOs corresponding to lone-pairs of the oxygen atoms. The results show that the inclusion of these electrons improves the initial EOM-CCSD/ELMO description, practically leading to the EOM-CCSD benchmark value.

Table 3. $n \rightarrow \pi^*$ excitation energies resulting from EOM-CCSD and EOM-CCSD/ELMO (with and without corrections to account for polarization response) calculations on formaldehyde and acrylamide in gas-phase and in presence of two water molecules.[(a)]

Calculation	formaldehyde		acrylamide	
	E_{ex} (eV)	ΔE_{ex} (eV)	E_{ex} (eV)	ΔE_{ex} (eV)
EOM-CCSD (full; with two water molecules)	4.158	//	5.561	//
EOM-CCSD (gas-phase; no water molecules)	3.962	-0.196	5.069	-0.492
EOM-CCSD/ELMO (two water molecules in the ELMO region)	4.168	0.010	5.543	-0.018
EOM-CCSD/ELMO + TDDFT correction (B3LYP)	4.128	-0.030	5.734	0.172
EOM-CCSD/ELMO + TDDFT correction (CAM-B3LYP)	4.158	0.000	5.527	-0.035
EOM-CCSD/ELMO + TDDFT correction (PBE0)	4.162	0.004	5.805	0.243
EOM-CCSD/ELMO + ELMOs selection	4.158	0.000	5.560	-0.001

[(a)] The ΔE_{ex} discrepancies are computed with respect to the $n \rightarrow \pi^*$ excitation energies resulting from the full EOM-CCSD calculations on formaldehyde and acrylamide surrounded by two water molecules.

Analogous test calculations were carried out on acrylamide. Also in this case, the simple EOM-CCSD/ELMO computation with two water molecules treated at ELMO level almost allows the full recovery of the gap between the $n \rightarrow \pi^*$ excitation energies obtained at full EOM-CCSD level in gas-phase and in presence of the two surrounding water molecules, with the discrepancy that decreases in absolute value from 0.492 eV to 0.018 eV. Unfortunately, in this situation, the TDDFT corrections do not improve the original EOM-CCSD/ELMO description. In fact, regardless of the

chosen functional, the deviation from the benchmark values always increases, in two cases even above the chemical accuracy threshold (0.172 eV and 0.243 eV for the B3LYP and PBE0 functionals, respectively). On the contrary, following the same procedure used for formaldehyde, the inclusion of the proper set of electrons in the QM region enables to practically recover the reference EOM-CCSD value, with a discrepancy reduced to only -0.001 eV.

To further show the performances of the new embedded EOM-CCSD technique in capturing the effects of the environment, in Figure 6 we also reported how the $n \rightarrow \pi^*$ excitation energies of formaldehyde (see Figure 6A) and acrylamide (see Figure 6B) obtained from EOM-CCSD/ELMO, TDDFT and TDHF calculations vary when the number of solvent water molecules increases from 2 to 30. It is easy to observe that the obtained trends are practically analogous for all the methods considered in our computations, thus confirming the capability of the new EOM-CCSD/ELMO approach in properly capturing the effects of the surrounding molecules on the local electronic transitions. Furthermore, from the inset of Figure 6 we can also notice that, in the cases in which the number of solvent molecules is small enough to easily perform full EOM-CCSD calculations (i.e., from two to five water molecules), both the EOM-CCSD(0)/ELMO and the EOM-CCSD(2)/ELMO computations provide excitation energies that perfectly agree with the reference ones (i.e., always within the threshold of chemical accuracy; see Tables S9-S10 in the Supporting Information for the actual values of the obtained excitation energies). This proves again that the new embedding EOM-CCSD/ELMO approach can be indeed used to reliably extend the range of applicability of the parent EOM-CCSD technique, without significantly affecting the accuracy of the results, but significantly reducing the computational cost.

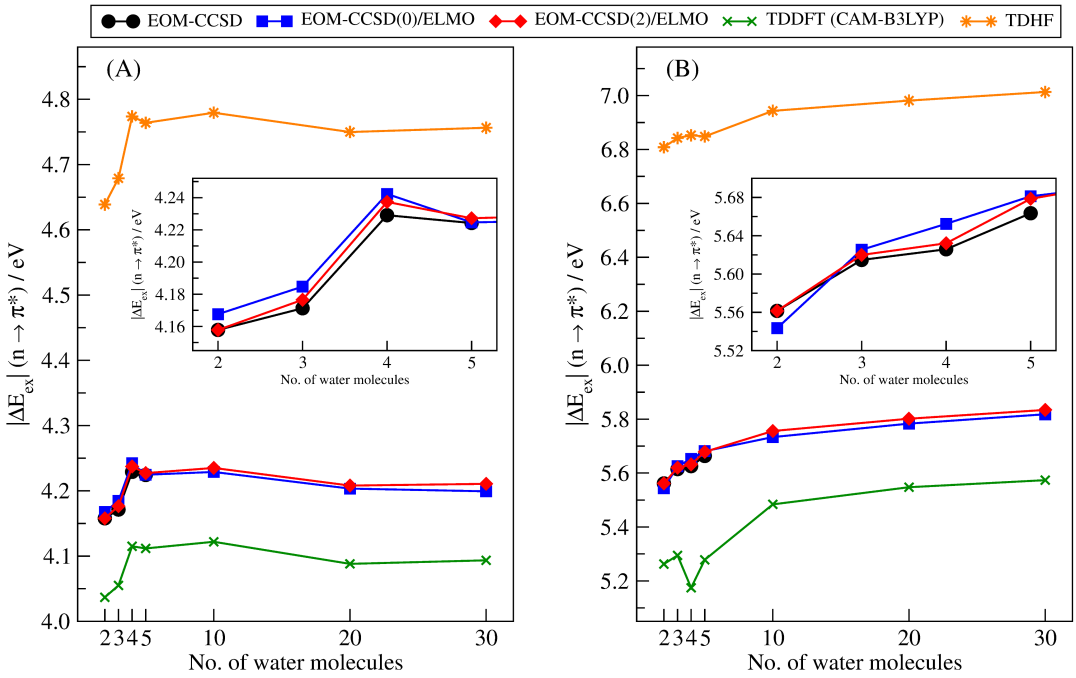

Figure 6. $n \rightarrow \pi^*$ excitation energies obtained at EOM-CCSD(0)/ELMO (no water molecules in the QM region), EOM-CCSD(2)/ELMO (two water molecules in the QM subsystem), full EOM-CCSD (when possible), TDDFT (CAM-B3LYP functional) and TDHF levels for solvated (A) formaldehyde and (B) acrylamide as the number of surrounding water molecules is gradually increased from 2 to 30; the inset highlights the EOM-CCSD(0)/ELMO, EOM-CCSD(2)/ELMO and full EOM-CCSD trends from 2 to 5 water molecules.

IV. CONCLUSIONS

In this work we have shown and tested the coupling of the recently developed QM/ELMO embedding approach to the accurate EOM-CCSD method, with the final goal of extending the applicability of the latter to the investigation of local excited-states in extended systems. All the validation tests have shown that treating only a small subsystem at EOM-CCSD level is generally enough to obtain results that agree with the fully quantum mechanical ones within the limit of chemical accuracy, with the additional advantage of a definitely lower computational cost. This was observed for both covalent and non-covalent boundaries between the active (QM) and environment (ELMO) regions.

Moreover, despite the use of only a non-flexible embedding potential given by transferred and frozen extremely localized molecular orbitals, the test calculations also showed that the novel EOM-CCSD/ELMO strategy is able to satisfactorily take into account the effects of the environment, whose description can be further improved through the suitable selection of ELMOs (and, consequently, of the associated electrons) to be included in the quantum mechanical subsystem. In this context, future improvements are already planned as, for instance, the exploitation of the virtual extremely localized molecular orbitals already available in the ELMO libraries to introduce polarizable embedding potentials that will enable to take into account both ground state polarization and polarization response effects more flexibly.

Finally, given the promising preliminary results obtained through the EOM-CCSD/ELMO and the related TDDFT/ELMO[62] techniques, the extension of the QM/ELMO embedding approach to other quantum chemical methods for the treatment of excited-states (e.g., CASSCF, CASPT2 or ΔSCF strategies) is also envisaged in the near future.

ASSOCIATED CONTENT

Supporting Information. Figure S1 depicting solvated formaldehyde and acrylamide (solute surrounded by thirty water molecules). Figures S2 and S3 showing the NTO analysis associated with the full EOM-CCSD calculations (first three excited-states) on 1-octene and octanoic acid, respectively. Tables S1 and S2 respectively reporting the EOM-CCSD/ELMO and EOM-CCSD excitation energies and oscillator strengths obtained for the first three excited-states of 1-octene and octanoic acid. Tables S3 and S4 respectively giving the EOM-CCSD/ELMO and EOM-CCSD $n \rightarrow \pi^*$ excitation

energies and oscillator strengths obtained for solvated formaldehyde, acetaldehyde, acrolein and acrylamide. Tables S5-S8 reporting the computational timings for the EOM-CCSD/ELMO and EOM-CCSD calculations on octanoic acid, solvated formaldehyde, solvated acetaldehyde and solvated acrolein. Tables S9 and S10 showing the $n \rightarrow \pi^*$ excitation energies obtained at different levels of theory (EOM-CCSD(0)/ELMO, EOM-CCSD(2)/ELMO, full EOM-CCSD (when possible), TDDFT (CAM-B3LYP functional) and TDHF) for formaldehyde and acrylamide, respectively, by increasing the number of surrounding water molecules from 2 to 30.

AUTHOR INFORMATION

Notes

The authors declare no competing financial interests.

ACKNOWLEDGEMNTS

The French Research Agency (ANR) is gratefully acknowledged for financial support of this work through the Young Research Project *QuMacroRef* (Grant No. ANR-17-CE29-0005-01). The High-Performance Computing Center *EXPLOR* of the University of Lorraine is thanked for providing computing time through the projects 2019CPMXX0966, 2019CPMXX0886 and 2019CPMXX1332. Fabien Pascale is also acknowledged for the set-up and maintenance of our local cluster, which was used to perform most of the calculations reported in this paper.

REFERENCES

[1] Jones, R. O.; Gunnarsson, O. The density functional formalism, its applications and prospects. *Rev. Mod. Phys.* **1989**, *61*, 689-746.

[2] Gavnholt, J.; Olsen, T.; Engelund, M.; Schiøtz, J. Δ self-consistent field method to obtain potential energy surfaces of excited molecules on surfaces. *Phys. Rev. B* **2008**, 075441.

[3] Gilbert, A. T. B.; Besley, N. A.; Gill, P. M. W. Self-Consistent Field Calculations of Excited States Using the Maximum Overlap Method (MOM). *J. Phys. Chem. A* **2008**, *112*, 13164-13171.

[4] Barca, G. M. J.; Gilbert, A. T. B.; Gill, P. M. W. Simple Models for Difficult Electronic Excitations. *J. Chem. Theory Comput.* **2018**, *14*, 1501-1509

[5] Buenker, R. J.; Peyerimhoff, S. D. CI method for the study of general molecular potentials. *Theor. Chim. Acta* **1968**, *12*, 183-199.

[6] Roos, B. O.; Taylor, P. R.; Siegbahn, P. E. M. A complete active space SCF method (CASSCF) using a density matrix formulated super-CI approach. *Chem. Phys.* **1980**, *48*, 157-173.

[7] Andersson, K.; Malmqvist, P. A.; Roos, B. O.; Sadlej, A. J.; Wolinski, K. Second-order perturbation theory with a CASSCF reference function. *J. Phys. Chem.* **1990**, *94*, 5483-5488.

[8] Rowe, D. J. Equations-of-Motion Method and the Extended Shell Model. *Rev. Mod. Phys.* **1968**, *40*, 153-166.

[9] Mukherjee, D.; Mukherjee, P. K. A response-function approach to the direct calculation of the transition-energy in a multiple-cluster expansion formalism. Chem. Phys. **1979**, *39*, 325-335.

[10] Sekino, H.; Bartlett, R. J. A linear response, coupled-cluster theory for excitation energy. *Int. J. Quantum Chem.* **1984**, *26*, 255-565.

[11] Dalgaard, E.; Monkhorst, H. J. Some aspects of the time-dependent coupled-cluster approach to dynamic response functions. *Phys. Rev. A* **1983**, *28*, 1217-1222.

[12] Del Bene, J. E.; Ditchfield, R.; Pople, J. A. Self-Consistent Molecular Orbital Methods. X. Molecular Orbital Studies of Excited States with Minimal and Extended Basis Sets. *J. Chem.Phys.* **1971**, *55*, 2236-2241.

[13] Runge, E.; Gross, E. K. U. Density-Functional Theory for Time- Dependent Systems. *Phys. Rev. Lett.* **1984**, *52*, 997-1000.

[14] Petersilka, M.; Gossmann, U. J.; Gross, E. K. U. Excitation Energies from Time-Dependent Density-Functional Theory. *Phys. Rev. Lett.* **1996**, *76*, 1212-1215.

[15] Casida, M. E. In *Recent Advances in Density Functional Methods, Part I*; Dong, D. P., Ed.; Recent Advances in Computational Chemistry; World Scientific: Singapore, 1995; pp 155-192.

[16] Adamo, C.; Jacquemin, D. The calculations of excited-state properties with Time-Dependent Density Functional Theory. *Chem. Soc. Rev.* **2013**, *42*, 845-856.

[17] Dreuw, A.; Head-Gordon, M. Failure of time-dependent density functional theory for long-range charge-transfer excited states: the zincbacteriochlorin-bacteriochlorin and bacteriochlorophyll-spher-oidene complexes. *J. Am. Chem. Soc.* **2004**, *126*, 4007-4016.

[18] Stanton, J. F.; Bartlett, R. J. The equation of motion coupled cluster method. A systematic biorthogonal approach to molecular excitation energies, transition probabilities, and excited state proper- ties. *J. Chem. Phys.* **1993**, *98*, 7029-7039.

[19] Krylov, A. I. Equation-of-motion coupled-cluster methods for open-shell and electronically excited species: The hitchhiker's guide to Fock space. *Annu. Rev. Phys. Chem.* **2008**, *59*, 433.

[20] Korona, T.; Werner, H.-J. Local treatment of electron excitations in the EOM-CCSD method. *J. Chem. Phys.* **2003**, *118*, 3006-3019.

[21] Baudin, P.; Kristensen, K. LoFEx-A local framework for calculating excitation energies: Illustrations using RI-CC2 linear response theory. *J. Chem. Phys.* **2016**, *144*, 224106.

[22] Höfener, S.; Klopper, W. Natural transition orbitals for the calculation of correlation and excitation energies. *Chem. Phys. Lett.* **2017**, *679*, 52-59.

[23] Dutta,A. K.; Neese,F.; Izsák, R. Towards a pair natural orbital coupled cluster method for excited states. *J. Chem. Phys.* **2016**, *145*, 034102.

[24] Baudin, P.; Bykov, D.; Liakh, D.; Ettenhuber, P.; Kristensen, K. A local framework for calculating coupled cluster singles and doubles excitation energies (LoFEx-CCSD). *Mol. Phys.* **2017**, *115*, 2135-2144.

[25] Kaliman, I. A.; Krylov, A. I. New algorithm for tensor contractions on multi-core CPUs, GPUs, and accelerators enables CCSD and EOM-CCSD calculations with over 1000 basis functions on a single compute node. *J. Comput. Chem.* **2017**, *38*, 842-853.

[26] Epifanovsky, E.; Zuev, D.; Feng, X.; Khistyaev, K.; Shao, Y.; Krylov, A. I. General implementation of the resolution-of-the-identity and Cholesky representations of electron repulsion integrals within coupled-cluster and equation-of-motion methods: theory and benchmarks. *J. Chem. Phys.* **2013**, *139*, 134105.

[27] Caricato, M. Absorption and Emission Spectra of Solvated Molecules with the EOM-CCSD-PCM Method. *J. Chem. Theory Comput.* **2012**, *8*, 4494−4502.

[28] Caricato, M. Exploring Potential Energy Surfaces of Electronic Excited States in Solution with the EOM-CCSD-PCM Method. *J. Chem. Theory Comput.* **2012**, *8*, 5081−5091.

[29] Caricato, M.; Lipparini, F.; Scalmani, G.; Cappelli, C.; Barone, V. Vertical Electronic Excitations in Solution with the EOM-CCSD Method Combined with a Polarizable Explicit/Implicit Solvent Model. *J. Chem. Theory Comput.* **2013**, *9*, 3035−3042.

[30] Haldar, S.; Dutta, A. K. A Multilayer Approach to the Equation of Motion Coupled-Cluster Method for the Electron Affinity. *J. Phys. Chem. A* **2020**, *124*, 3947-3962.

[31] Dutta, A. K.; Saitow, M.; Demoulin, B.; Neese, F.; Izsák, R. A Domain-Based Local Pair Natural Orbital Implementation of the Equation of Motion Coupled Cluster Method for Electron Attached States. *J. Chem. Phys.* **2019**, *150*, 164123.

[32] Manby, F. R.; Stella, M.; Goodpaster, J. D.; Miller, T. F., III. A simple, exact density-functional theory embedding scheme. *J. Chem. Theory Comput.* **2012**, *8*, 2564−2568.

[33] Barnes, T. A.; Goodpaster, J. D.; Manby, F. R.; Miller, T. F., III. Accurate basis-set truncation for wavefunction embedding. *J. Chem. Phys.* **2013**, *139*, 024103.

[34] Goodpaster, J. D.; Barnes, T. A.; Manby, F. R.; Miller, T. F., III. Accurate and systematically improvable density functional theory embedding for correlated wave functions. *J. Chem. Phys.* **2014**, *140*, 18A507.

[35] Lee, S. J. R.; Welborn, M.; Manby, F. R.; Miller, T. F., III. Projection-Based Wavefunction-in-DFT Embedding. *Acc. Chem. Res.* **2019**, *52*, 1359-1368.

[36] Bennie, S. J.; Curchod, B. F. E.; Manby, F. R.; Glowacki, D. R. Pushing the Limits of EOM-CCSD with Projector-Based Embedding for Excitation Energies. *J. Phys. Chem. Lett.* **2017**, *8*, 5559-5565.

[37] Chulhai, D. V.; Goodpaster, J. D. Improved Accuracy and Efficiency in Quantum Embedding though Absolute Localization. *J. Chem. Theory Comput.* **2017**, *13*, 1503-1508.

[38] Chulhai, D. V.; Goodpaster, J. D. Projection-Based Correlated Wave Function in Density Functional Theory Embedding for Periodic Systems. *J. Chem. Theory Comput.* **2018**, *14*, 1928−1942.

[39] Wen, X.; Graham, D. S.; Chulhai, D. V.; Goodpaster, J. D. Absolutely Localized Projection-based Embedding for Excited-States. *J. Chem. Theory. Comput.* **2020**, *16*, 385-398.

[40] Chulhai, D. V.; Jensen, L. External orthogonality in subsystem time-dependent density functional theory. *Phys. Chem. Chem. Phys.* **2016**, *18*, 21032-21039.

[41] Tölle, J.; Böckers, M.; Neugebauer, J. Exact subsystem time- dependent density-functional theory. *J. Chem. Phys.* **2019**, *150*, 181101.

[42] Scholz, L.; Tölle, J.; Neugebauer, J. Analysis of environment response effects on excitation energies within subsystem-based time-dependent density-functional theory. *Int. J. Quantum Chem.* **2020**, e26213, DOI: 10.1002/qua.26213.

[43] de Lima Batista, A. P.; de Oliveira-Filho, A. G. S.; Galembeck, S. E. Photophysical properties and the NO photorelease mechanism of a ruthenium nitrosyl model complex investigated using the CASSCF-in-DFT embedding approach. *Phys. Chem. Chem. Phys.* **2017**, *19*, 13860-13867.

[44] Macetti, G.; Genoni, A. Quantum Mechanics/Extremely Localized Molecular Orbital Method: A Fully Quantum Mechanical Embedding Approach for Macromolecules. *J. Phys. Chem. A* **2019**, *123*, 9420-9428.

[45] Macetti, G.; Wieduwilt, E. K.; Assfeld, X.; Genoni. A. Localized Molecular Orbital-Based Embedding Scheme for Correlated Methods. *J. Chem. Theory Comput.* **2020**, *16*, 3578-3596.

[46] Stoll, H.; Wagenblast, G.; Preuss, H. On the Use of Local Basis Sets for Localized Molecular Orbitals. *Theor. Chim. Acta* **1980**, *57*, 169−178.

[47] Fornili, A.; Sironi, M.; Raimondi, M. Determination of Extremely Localized Molecular Orbitals and Their Application to Quantum Mechanics/Molecular Mechanics Methods and to the Study of Intramolecular Hydrogen Bonding. *J. Mol. Struct. (THEOCHEM)* **2003**, *632*, 157-172.

[48] Sironi, M.; Genoni, A.; Civera, M.; Pieraccini, S.; Ghitti, M. Extremely Localized Molecular Orbitals: Theory and Applications. *Theor. Chem. Acc.* **2007**, *117*, 685-698.

[49] Meyer, B.; Guillot, B.; Ruiz-Lopez, M. F.; Genoni, A. Libraries of Extremely Localized Molecular Orbitals. 1. Model Molecules Approximation and Molecular Orbitals Transferability. *J. Chem. Theory. Comput.* **2016**, *12*, 1052-1067.

[50] Meyer, B.; Guillot, B.; Ruiz-Lopez, M. F.; Jelsch, C.; Genoni, A. Libraries of Extremely Localized Molecular Orbitals. 2. Comparison with the Pseudoatoms Transferability. *J. Chem. Theory. Comput.* **2016**, *12*, 1068-1081.

[51] Genoni, A; Sironi, M. A Novel Approach to Relax Extremely Localized Molecular Orbitals: the Extremely Localized Molecular Orbital-Valence Bond Method. *Theor. Chem. Acc.* **2004**, *112*, 254-262.

[52] Genoni, A.; Fornili, A.; Sironi, M. Optimal Virtual Orbitals to Relax Wave Functions Built Up with Transferred Extremely Localized Molecular Orbitals. *J. Comput. Chem.* **2005**, *26*, 827-835.

[53] Genoni, A.; Ghitti, M.; Pieraccini, S.; Sironi, M. A novel extremely localized molecular orbitals based technique for the one-electron density matrix computation. *Chem. Phys. Lett.* **2005**, *415*, 256-260.

[54] Genoni, A.; Merz. K. M., Jr.; Sironi, M. A Hylleras functional based perturbative technique to relax extremely localized molecular orbitals. *J. Chem. Phys.* **2008**, *129*, 054101.

[55] Sironi, M.; Ghitti, M.; Genoni, A.; Saladino, G.; Pieraccini, S. DENPOL: A new program to determine electron densities of polypeptides using extremely localized molecular orbitals. *J. Mol. Struct. (THEOCHEM)* **2009**, *898*, 8-16.

[56] Meyer, B.; Genoni, A. Libraries of Extremely Localized Molecular Orbitals. 3. Construction and Preliminary Assessment of the New Databanks. *J. Phys. Chem. A* **2018**, *122*, 8965-8981.

[57] Malaspina, L. A.; Wieduwilt, E. K.; Bergmann, J.; Kleemiss, F.; Meyer, B.; Ruiz-López, M.-F.; Pal, R.; Hupf, E.; Beckmann, J.; Piltz, R. O.; Edwards, A. J.; Grabowsky, S.; Genoni, A. Fast and Accurate Quantum Crystallography: from Small to Large, from Light to Heavy. *J. Phys. Chem. Lett.* **2019**, *10*, 6973-6982.

[58] Culpitt, T.; Brorsen, K. R.; Pak, M. V.; Hammes-Schiffer, S. Multicomponent density functional theory embedding formulation. *J. Chem. Phys.* **2016**, *145*, 044106.

[59] Culpitt, T.; Brorsen, K. R.; Hammes-Schiffer, S. Communica- tion: Density functional theory embedding with the orthogonality constrained basis set expansion procedure. *J. Chem. Phys.* **2017**, *146*, 211101.

[60] Claudino, D.; Mayhall, N. J. Automatic Partition of Orbital Spaces Based on Singular Value Decomposition in the Context of Embedding Theories. *J. Chem. Theory Comput.* **2019**, *15*, 1053-1064.

[61] Philipp, D. M.; Friesner, R. A. Mixed Ab Initio QM/MM Modeling Using Frozen Orbitals and Tests with Alanine Dipeptide and Tetrapeptide. *J. Comput. Chem.* **1999**, *20*, 1468-1494.

[62] Macetti, G.; Genoni, A. Quantum Mechanics / Extremely Localized Molecular Orbital Embedding Strategy for Excited-States. 1. Coupling to Time-Dependent Density Functional Theory. *J. Chem. Theory Comput.*, submitted.

[63] Frisch, M. J.; Trucks, G. W.; Schlegel, H. B.; Scuseria, G. E.; Robb, M. A.; Cheeseman, J. R.; Scalmani, G.; Barone, V.; Mennucci, B.; Petersson, G. A.; Nakatsuji, H.; Caricato, M.; Li, X.; Hratchian, H. P.; Izmaylov, A. F.; Bloino, J.; Zheng, G.; Sonnenberg, J. L.; Hada, M.; Ehara, M.; Toyota, K.; Fukuda, R.; Hasegawa, J.; Ishida, M.; Nakajima, T.; Honda, Y.; Kitao, O.; Nakai, H.; Vreven, T.; Montgomery, J. A., Jr.; Peralta, J. E.; Ogliaro, F.; Bearpark, M.; Heyd, J. J.; Brothers, E.; Kudin, K. N.; Staroverov, V. N.; Kobayashi, R.; Normand, J.; Raghavachari, K.; Rendell, A.; Burant, J. C.; Iyengar, S. S.; Tomasi, J.; Cossi, M.; Rega, N.; Millam, J. M.; Klene, M.; Knox, J. E.; Cross, J. B.; Bakken, V.; Adamo, C.; Jaramillo, J.; Gomperts, R.; Stratmann, R. E.; Yazyev, O.; Austin, A. J.; Cammi, R.; Pomelli, C.; Ochterski, J. W.; Martin, R. L.; Morokuma, K.; Zakrzewski, V. G.; Voth, G. A.; Salvador, P.; Dannenberg, J. J.; Dapprich, S.; Daniels, A. D.; Farkas, Ö.; Foresman, J. B.; Ortiz, J. V.; Cioslowski, J.; Fox, D. J. *Gaussian 09*, Revision D.01; Gaussian, Inc., Wallingford, CT, USA, 2009.

[64] Kluner, T.; Govind, N.; Wang, Y. A.; Carter, E. A. Periodic density functional embedding theory for complete active space self-consistent field and configuration interaction calculations: Ground and excited states. *J. Chem. Phys.* **2002**, *116*, 42-54.

[65] Guest, M. F.; Bush, I. J.; van Dam, H. J. J.; Sherwood, P.; Thomas, J. M. H.; van Lenthe, J. H.; Havenith, R. W. A.; Kendrick, J. The GAMESS-UK Electronic Structure Package: Algorithms, Developments and Applications. *Mol. Phys.* **2005**, *103*, 719−747.